Journal of Solid State Chemistry 184 (2011) 3221–3227

Contents lists available at SciVerse ScienceDirect

Journal of Solid State Chemistry

journal homepage: www.elsevier.com/locate/jssc

Seeking the optimal $LaTaO_4$:Eu phosphor

Grant C. Bleier, May Nyman*, Lauren E.S. Rohwer, Mark A. Rodriguez

Sandia National Laboratories, P.O. Box 5800, Albuquerque, NM 87185, United States

ARTICLE INFO

Article history:
Received 28 June 2011
Received in revised form
30 September 2011
Accepted 4 October 2011
Available online 14 October 2011

Keywords:
Orthotantalate
Rare-earth
Europium
Phosphor
Solid-state lighting

ABSTRACT

Lanthanum orthotantalate, $LaTaO_4$, is an excellent host lattice for rare-earth luminescent ions such as Eu^{3+} for red emission. However, there are multiple *RE*TaO_4 (*RE*=rare earth) polymorphs, and the stability of these is controlled predominantly by the RE-radius. Thus it is difficult to obtain a pure phase of $LaTaO_4$:Eu as Eu concentration and consequently the *RE* radius is varied. We recently reported a 'soft-chemical' route that allows crystallization of pure-phase $LaTaO_4$:Eu at temperatures as low as 800 °C. In the current report, we investigate polymorph evolution and Eu emission as a function of Eu concentration and annealing temperature. We obtain a maximum quantum yield (QY) of 83% at the highest Eu substitution (25%) for which the low temperature orthorhombic (*Pbca*) polymorph is stable. Therefore, QY is not limited necessarily by concentration quenching; rather it is limited by polymorph stability as the RE-radius decreases with increasing Eu substitution.

1. Introduction

Europium phosphors are exceedingly important in a variety of technologies including authenticity tagging, fluorescent lamps, and the emerging LED-based solid-state lighting [1]. It is well-known that the Euro banknote (official currency of the European Union) emits red under a UV-lamp, due to the presence of a proprietary europium compound as an anti-counterfeiting measure. Fluorescent lamps contain alkaline-earth aluminates or phosphates doped with Eu^{2+} for blue emission (i.e. BAM:Eu; barium magnesium aluminate) and red-emitting Eu^{3+}-doped yttrium oxide. Yttrium oxysulfide doped with Eu^{3+} emits red and is used in CRT displays. Finally, a recently discovered class of phosphors, the alkaline earth nitridosilicates doped with Eu^{2+} [2–6] emit yellow–green or orange–red when excited by a blue LED, and has been found that it can be used in improving color rendering for solid-state lighting (SSL) devices. Every application has a demanding list of requirements for the phosphor material including excitation and emission at wavelengths that are optimal for a given device, high quantum yield (QY), good luminous efficacy of radiation (LER) and minimal thermal quenching.

We and others have recently focused on the development of tantalate and niobate materials as host lattices for Eu^{3+} emission [7–11]. Soft-chemical methods are of particular interest, in that niobates and tantalates are incredibly refractory, generally requiring heating temperatures of 1600 °C to obtain full crystallinity. Both hydrothermal [7,8] and flux [9] syntheses are good approaches; our focus has been largely hydrothermal. In general, our rare-earth tantalate materials feature sharp Eu^{3+} emission at 610 nm when excited with blue light (λ∼465 nm); and they have low thermal quenching, due to the very stable and robust nature of tantalate lattices [7,8]. We have found that large concentrations of Eu^{3+} can be incorporated into these host lattices without decrease in QY due to concentration quenching. In this regard, they are similar to luminescent rare-earth molybdates [12–14], tungstates [15,16], and niobates and tantalates[17,18] in which Eu is a stoichiometric component rather than a dopant. It is generally understood that structural features such as long Eu–Eu distances or lattice bond angles that result in difficulty in energy transfer are responsible for minimal concentration quenching [19,20].

We reported prior a new low-temperature orthorhombic polymorph of $LaTaO_4$ that can be obtained only by soft-chemical synthesis. The low-temperature polymorph does not form directly in the hydrothermal reaction: rather $La_2Ta_2O_7(OH)_2$ forms hydrothermally [21], and is converted into $LaTaO_4$ by heating to 850 °C [7]. Upon further heating to 1100 °C and higher, the low temperature polymorph converts completely into a high temperature polymorph [7]. When the hydrothermal synthesis is carried out with substitution of Eu on the La-site, $La_2Ta_2O_7(OH)_2$:Eu is formed and likewise converted into $LaTaO_4$:Eu, where the low-temperature, orthorhombic polymorph exhibits higher QY of the Eu emission than the higher temperature monoclinic polymorph [7].

In this work, we further explore the synthesis and luminescence characteristics of $LaTaO_4$:Eu polymorphs. In addition to investigating the phases with higher Eu concentration, we also compare the hydrothermal synthesis to traditional solid-state processing. QY, morphology and structural changes of $LaTaO_4$:Eu polymorphs are

* Corresponding author.
E-mail address: mdnyman@sandia.gov (M. Nyman).

0022-4596/$ - see front matter © 2011 Elsevier Inc. All rights reserved.
doi:10.1016/j.jssc.2011.10.008

documented as a function of Eu concentration. There are several polymorphs of $RETaO_4$ (RE=rare earth) and their stability is strongly dependent on the RE radius (changes linearly with La:Eu ratio). This was also noted prior to comparing the formation of $LaTaO_4$, $PrTaO_4$ and $NdTaO_4$ polymorph as from their respective $La_2Ta_2O_7(OH)_2$, $Pr_2Ta_2O_7(OH)_2$ and $Nd_2Ta_2O_7(OH)_2$ precursors [22]. Thus in the $LaTaO_4$:Eu system, QY optimization is not necessarily limited by concentration quenching, but more likely the interrelated effects of rare-earth radius as a function of Eu concentration and polymorph stability. The coincidence of several polymorphs for some Eu concentrations and annealing temperatures quickly renders QY optimization difficult to understand and control. However, we have empirically determined optimal Eu concentration to be ~25%: the maximum concentration at which the low temperature polymorph dominated, and an impressive QY of 83% was obtained.

2. Materials and methods

2.1. Synthesis

2.1.1. $LaTaO_4$:Eu via 'soft chemistry'

$LaTaO_4$:Eu via the hydrothermal route was synthesized using methods, which we have previously reported [7,21]. $La_2Ta_2O_7(OH)_2$:Eu is synthesized hydrothermally. Lanthanum nitrate $La(NO_3)_3 \cdot 6H_2O$ (Aldrich, FW=433.02) (0.411 g for 5% Eu-doped, 0.389 g for 10% Eu-doped, 0.346 g for 20%, 0.325 g for 25%, 0.303 g for 30%, 0.281 g for 35%, and 0.259 g for 40%) and europium nitrate, $Eu(NO_3)_3 \cdot 5H_2O$ (Aldrich, FW=428.05) (0.021 g for 5% Eu-doped, 0.043 g for 10% Eu-doped, 0.086 g for 20%, 0.107 g for 25%, 0.128 g for 30%, 0.150 g for 35%, and 0.171 g for 40%) are combined in proportional amounts and dissolved in 12.5 mL of DI (deionized) H_2O. The total amount of lanthanum and europium salt is 1.0 mmol. Potassium citrate (0.357 g, 1.0 mmol) is dissolved separately, also in 12.5 mL of DI H_2O and added drop-wise into the dissolved lanthanide salt solution while stirring vigorously. Addition of the potassium citrate produces a thick white precipitate, which then redissolves after thirty drops of 4 M aqueous KOH solution is added. The potassium peroxotantalate salt $K_3[TaO_2]_4$ was synthesized as reported prior [23]. In 25 mL of DI H_2O, 0.426 g (1.0 mmol) of the tantalate salt is dissolved and combined with the lanthanide citrate solution in a 125 mL Teflon liner for a Parr reactor. The Parr reactor is placed in a 225 °C oven for 3 days. After cooling, the white microcrystalline product is collected via centrifugation at 4500 rpm in a Beckman-Coulter Allegra® X-22 R Centrifuge for 10 min. The top H_2O layer is decanted and this process is repeated for ~2–3 times with methanol to remove remaining H_2O, KOH, and citrate. $LaTaO_4$:Eu is formed by annealing the dry powder $La_2Ta_2O_7(OH)_2$:Eu in a 75 mL crucible at 900 °C for 2 h. Alternatively higher temperature annealing is carried out by pressing the dry powder $La_2Ta_2O_7(OH)_2$:Eu into a pellet and annealing the pellet in a 75 mL crucible at 1150 °C for 2 h.

2.1.2. Solid-state synthesis of $LaTaO_4$:Eu

The reagents for these preparations included tantalum oxide, Ta_2O_5 (Acros, FW=441.89), europium nitrate, $Eu(NO_3)_3 \cdot 5H_2O$ (Aldrich, FW=428.05) and lanthanum nitrate $La(NO_3)_3 \cdot 6H_2O$ (Aldrich, FW=433.02). These were combined with alcohol (isopropanol) plus YSZ (yttria-stabilized zirconia) mixing beads in a 60 mL test tube or centrifuge tube. The alcohol-precursor slurry was then shaken on a Turbula® (General Mills Inc.) for 40–90 min. The resulting slurry mixture was poured through a Buchner funnel to remove the mixing beads, into a 75 mL crucible. The isopropanol was removed *in-vacuo* and then the powder was heated at 900 °C for 5 h. The resulting powder was remixed in the same method described above, then pressed into a pellet and heated at 1150 °C for 5 h. The pellet was reground into a powder using a mortar and pestle, remixed as described above; and again pressed into a pellet and heated at 1150 °C for 5 h: pelletization and heating were carried out a total of four times. The pellet was then ground into a fine powder for subsequent characterization. Two compositional variations were synthesized: 25%-Eu substituted $LaTaO_4$ and 30%-Eu substituted $LaTaO_4$. For both, 1 g tantalum oxide (4.5 mmol) was utilized. For the former, 0.484 g europium nitrate (1.13 mmol) and 1.469 g lanthanum nitrate (3.39 mmol) were utilized, and for the latter 0.581 g europium nitrate (1.36 mmol) and 1.372 g lanthanum nitrate (3.17 mmol) were utilized.

2.2. Characterization

All $LaTaO_4$:Eu were characterized by powder X-ray diffraction. X-ray powder diffraction for phase identification was performed with a Bruker D8 Advance diffractometer in Bragg–Brentano geometry with Ni-filtered Cu $K\alpha$ radiation. For samples requiring unit cell parameter refinement, the powders were mixed with Si (SRM 640c) as an internal standard prior to data collection. Lattice parameter refinement was carried out using the software package JADE (ver. 9.1). Full pattern fitting was attempted to identify the different polymorphic components; however these attempts were not successful due to poor crystallinity in the case of the materials obtained by solid-state processing, and strong preferred orientation in the case of the 'soft-chemical' materials. The Scanning Electron Microscopy and Energy Dispersive Spectroscopy (SEM-EDS) were performed on a Zeiss Supra 55VP field emission microscope equipped with an Oxford X-MAX 80 mm^2 detector.

The photoluminescence (PL) emission and excitation spectra were collected using a Horiba Jobin-Yvon Fluorolog-3 double-grating/double-grating Fluorescence Spectrophotometer. Powder measurements were made by orienting the sample 11° from the incident beam and detecting the emitted light from the front face of the sample. The excitation spectra were collected over the wavelength range of 250–550 nm, with the emission monitored at 614 nm. A complete instrumental correction was performed on all spectra, including corrections for the wavelength-dependent PMT response and grating efficiencies, among other factors. Absolute quantum yield measurements were made by exciting the samples with diffuse light (464 nm) inside an integrating sphere, as described prior [7,24]. Error on these measurements is ~0.6% based on prior studies [24].

3. Results and discussion

In our various $LaTaO_4$:Eu materials, we observe several polymorphs of $LaTaO_4$ including monoclinic $P2_1/c$ [25], orthorhombic $Cmc2_1$ [26] as well as our recently reported orthorhombic $Pbca$ [7]. Fig. 1 shows representative diffraction patterns for the $LaTaO_4$:Eu formed by solid-state processing, and from annealing of the hydrothermally-obtained $La_2Ta_2O_7(OH)_2$:Eu precursor powder, as well as calculated diffraction patterns of the $RETaO_4$ (RE=rare earth) polymorphs. In every case, there is 25% substitution of Eu for La, or the Eu:La ratio is 1:3. Since the calculated diffraction patterns are obtained from pure $RETaO_4$ phases, they all have different d-spacings (thus different 2-θ peak positions) than the 25%-Eu substituted lanthanum tantalates. Therefore the observed and calculated diffraction patterns do not match, rather they are intended as a guide for polymorph identification.

We note that the $LaTaO_4$:Eu powder obtained from traditional solid-state processing possesses rather poor crystallinity, as indicated by the low signal:noise (Fig. 1a), even though it had been processed via a total of five remixing and heating steps.

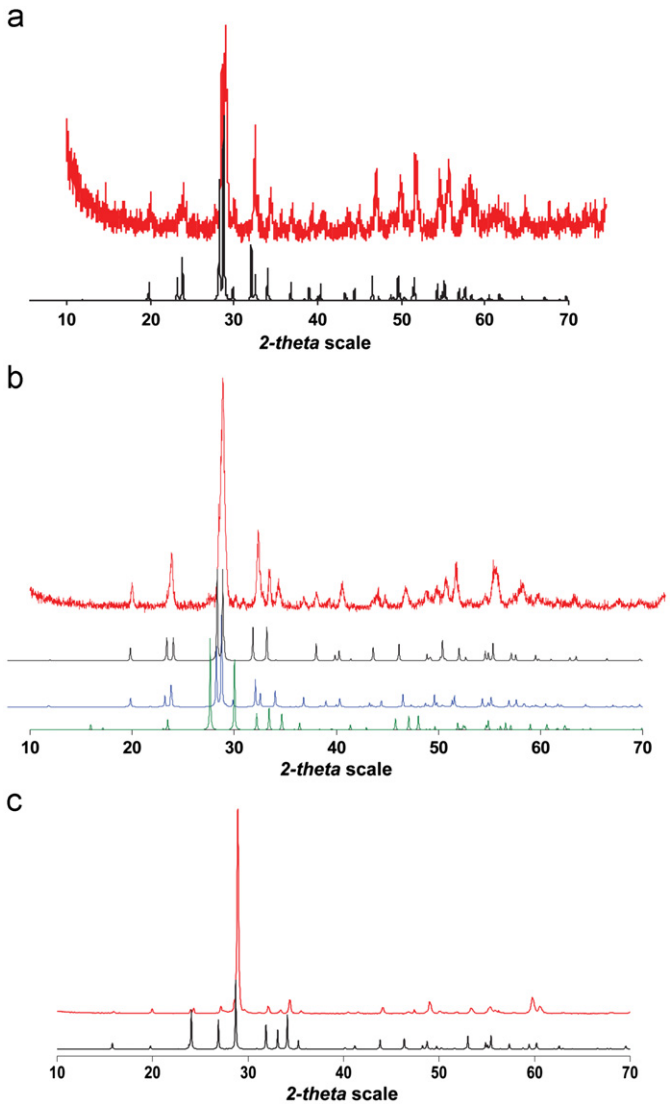

Fig. 1. (a) Observed (red) X-ray powder diffraction pattern for $LaTaO_4$:Eu (25% Eu) formed by solid-state processing at 1150 °C. Calculated diffraction pattern (black) for monoclinic $P2_1/c$ $LaTaO_4$. (b) Observed (red) X-ray powder diffraction pattern for $LaTaO_4$:Eu (25% Eu) formed by annealing hydrothermal product at 1150 °C. Calculated diffraction patterns for monoclinic $P2_1/c$ (blue) and orthorhombic $Cmc2_1$ (black) $LaTaO_4$ and monoclinic $P2/c$ $SmTaO_4$. (c) Observed (red) diffraction pattern of $LaTaO_4$:Eu (25%Eu) formed from the hydrothermal product by annealing at 900 °C. Calculated diffraction pattern (black) for orthorhombic *Pbca* $LaTaO_4$. (For interpretation of the references to color in this figure legend, the reader is referred to the web version of this article.)

Ideally rare-earth tantalates are annealed at >1500 °C to obtain suitable crystallinity [27]. However, the heating was executed at the relatively low temperature of 1150 °C, for direct comparison to the annealed, hydrothermal products, which is probably the reason for the poor crystallinity. Furthermore, elevated temperature-annealing of laboratory-scale phosphor powders (several gram quantities) result in ever-increasing difficulties with maintaining phase and compositional purity, due to increasing reactivity with substrates and vessels for heating. The X-ray diffraction pattern of this $LaTaO_4$:Eu obtained from solid-state processing indicates it is predominantly the monoclinic $P2_1/c$ polymorph. Fig. 1b shows the X-ray diffraction pattern of $La_2Ta_2O_7(OH)_2$:Eu (25%) precursor powder that was pressed into a pellet and annealed at 1150 °C for 2 h. It was initially pressed into a pellet prior to annealing for two reasons: (1) for more direct comparison to the solid-state $LaTaO_4$:Eu, and (2) to minimize contact with its annealing crucible, which potentially results in contamination that is detrimental to luminescence properties. Its signal:noise is somewhat better than that of the solid-state $LaTaO_4$:Eu. However, it is clearly not phase-pure; monoclinic $P2_1/c$ [25] and orthorhombic $Cmc2_1$ [26] polymorphs are observed. Furthermore, there are some peaks that match most closely the monoclinic $P2/c$ polymorph that is more stable for the smaller lanthanides [25], and the calculated diffraction pattern for $SmTaO_4$ is shown in Fig. 1b (in green) for comparison. There may be other $RETaO_4$ phases present as well; but the combination of poor signal:noise and overlapping peaks between polymorphs renders quantification of this result difficult. In contrast, well-crystalline, monoclinic $P2_1/c$ polymorph $LaTaO_4$ cleanly forms at 1150 °C from the $La_2Ta_2O_7(OH)_2$ precursor that contains no substitution of Eu; and this is shown in Fig. 2. Fig. 1c shows $LaTaO_4$:Eu (25%) formed from heating the $La_2Ta_2O_7(OH)_2$:Eu precursor powder at 900 °C. It is pure, well-crystalline orthorhombic *Pbca* $RETaO_4$ polymorph.

The reason for obtaining a mixture of $LaTaO_4$:Eu polymorphs when substituting a substantial amount of Eu for La ($>25\%$, discussed later) is directly related to the rare-earth radii. It is well-documented that the lanthanide contraction results in change in solid-state structure with RE^{3+} radius [25]. We observed this prior while investigating the thermal evolution from $RE_2Ta_2O_7(OH)_2$ to $RETaO_4$ for RE=Pr and Nd [22]. (Ce^{3+} is unstable under the alkaline hydrothermal synthesis conditions and converted to Ce^{4+}, so it was not studied extensively). While the La analog converts cleanly first to the *Pbca* polymorph and then to the $P2_1/c$ polymorph at 850 and 1150 °C, respectively, the Nd and Pr analogs produced a complex mixture of phases, and pure polymorphs were never observed. Apparently at the boundary between larger and smaller lanthanides, there are multiple orthotantalate polymorphs that have comparable stability. Fig. 3 plots the 8-coordinate ionic radius of trivalent RE [28] for the $LaTaO_4$:Eu phases as a function of Eu substitution. This radius represents the fraction of the La–Eu in the $LaTaO_4$:Eu material:

For $La_xEu_{1-x}TaO_4$; rare-earth radius$=r_{La}(x)+r_{Eu}(1-x)$.

It is self-evident that the RE radius decreases linearly with increasing Eu substitution for La. Also plotted on the linear regression of Fig. 3 are: (1) the 8-coordinate ionic radii for the next two smaller RE; Ce and Pr, and (2) the RE radius for the composition of $LaTaO_4$:Eu (25%Eu) that gives the optimal QY for Eu-emission. We note that with Eu-substitution of 25% or less, we obtain predominantly orthorhombic *Pbca* $LaTaO_4$:Eu. However, above 25% we obtain a mixture of polymorphs. The 8-coordinate ionic radii of Ce^{3+} and Pr^{3+} are, respectively, the equivalent of the lanthanide radii of 18%-Eu substituted and 36%-Eu substituted

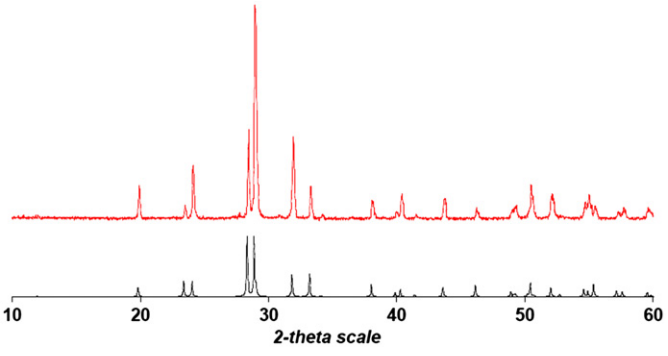

Fig. 2. Observed (red) X-ray powder diffraction pattern of monoclinic $P2_1/c$ polymorph of $LaTaO_4$ that cleanly forms at 1150 °C from the $La_2Ta_2O_7(OH)_2$ precursor that contains no substitution of Eu. Shown in black is the calculated diffraction pattern for this polymorph. (For interpretation of the references to color in this figure legend, the reader is referred to the web version of this article.)

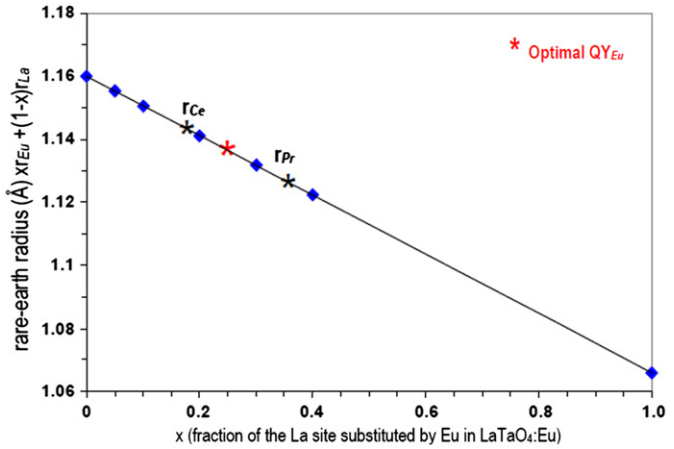

Fig. 3. The 8-coordinate ionic radii (RE^{3+}) for mixed Eu–La site as a function of %-Eu substitution in $LaTaO_4$:Eu. The red star denotes the 25% Eu substitution, at which optimal QY_{Eu} was obtained (83%). The 8-coordinate radii for Ce and Pr are also plotted for comparison (black stars, see text). (For interpretation of the references to color in this figure legend, the reader is referred to the web version of this article.)

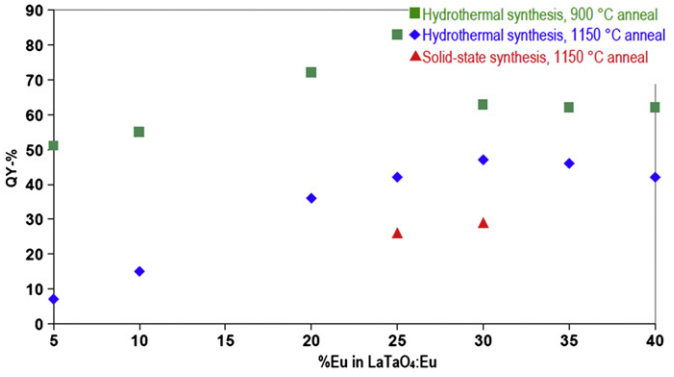

Fig. 4. Quantum Yield (QY) of Eu emission for $LaTaO_4$:Eu excited with blue light (464 nm) as a function of Eu-concentration and synthesis method. (Error on data points is ~0.6%.)

$LaTaO_4$:Eu. Since we know from prior study [22] that it is difficult to obtain a pure phase orthotantalate with *Ln*=Pr, it is not surprising that the higher concentration of Eu compromises the phase purity of these phosphor materials obtained at 900 °C. The mixtures of phases become more complex at higher annealing temperature (1150 °C) as illustrated in Fig. 1b. The reason for this may be two-fold: (1) perhaps the kinetic barrier for conversion between the different orthotantalate polymorphs decreases at higher annealing temperature, and (2) there may actually be some phase separation to Eu-rich phases and La-rich phases, based on the Ln-radius preference for different polymorphs.

The phase purity and polymorph preference as a function of Eu-concentration, annealing temperature and synthesis method (traditional solid-state processing vs. annealing of $La_2Ta_2O_7(OH)_2$:Eu) clearly affects the quantum yield (QY) of the europium emission, as illustrated in Fig. 4. The QY values trend:

$LaTaO_4$:Eu from $La_2Ta_2O_7(OH)_2$:Eu annealed at 900 °C >
$LaTaO_4$:Eu from $La_2Ta_2O_7(OH)_2$:Eu annealed at 1150 °C >
$LaTaO_4$:Eu from solid-state processing at 1150 °C

The 25%-Eu substituted $LaTaO_4$:Eu from $La_2Ta_2O_7(OH)_2$:Eu annealed at 900 °C provides the optimal Eu-emission with an impressive QY of 83%. Higher than 25% Eu-substitution results in a drop of QY to around 60%, likely because of the mixed polymorphs obtained as a function of decreasing RE^{3+}-radius. While concentration quenching could also be a factor, there is stronger evidence for change in polymorph being responsible for this trend. A similar trend is observed for $La_2Ta_2O_7(OH)_2$:Eu annealed at 1150 °C, but the maximum QY reached in this series is less than 50%. Finally, two $LaTaO_4$:Eu (Eu=25%, 30%) samples prepared from lanthanum nitrate, europium nitrate, and tantalum oxide by solid-state processing had QY values below 30%, much lower than the comparable $LaTaO_4$:Eu materials prepared from annealing of $La_2Ta_2O_7(OH)_2$:Eu. The explanations for this are apparent: poorer crystallinity (more structure defects) and possibly also incomplete homogenization of Eu and La in the crystalline lattices. This is clearly a case in which atomic-level mixing by 'soft-chemistry' has proven to produce materials with superior functionality because (1) rare-earth tantalates are incredibly refractory and therefore have very high crystallization temperatures, low diffusion rates of ions in their solid-state lattices, etc. and (2) we showed prior that the *Pbca* $LaTaO_4$ polymorph [7] obtained at lower temperature (900 °C) could only be obtained from $La_2Ta_2O_7(OH)_2$, and furthermore has better QY than the $P2_1/c$ polymorph obtained at 1150 °C. The unit cell volume and unit cell dimensions (*a*, *b*, and *c*) of *Pbca* $LaTaO_4$:Eu were determined by Rietveld refinement and are plotted as a function of Eu-concentration (Fig. 5a and b). The La:Eu ratio was determined by energy dispersive spectroscopy (EDS) compared to standards. The linear correlation between %Eu-substitution and unit cell

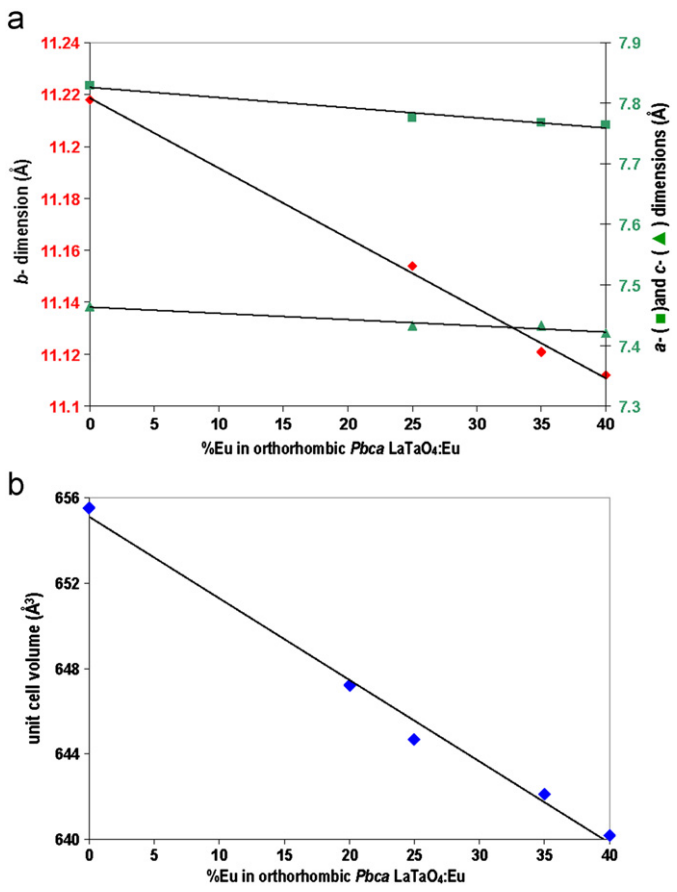

Fig. 5. (a) Unit cell parameters (Å) (*a*=green square, right axis; *b*=red diamond, left axis; and *c*=green triangle, right axis) of orthorhombic *Pbca* $LaTaO_4$:Eu as a function of Eu-concentration. (b) Unit cell volume (Å^3) of orthorhombic *Pbca* $LaTaO_4$:Eu as a function of Eu-concentration. (For interpretation of the references to color in this figure legend, the reader is referred to the web version of this article.)

parameters is excellent, small observed deviations from linearity are likely introduced by error in the EDS analyses. This suggests the bulk La:Eu ratio of the synthesis product (determined by EDS) corresponds with the amount provided in the experiment, and the La and Eu does not preferentially segregate into different $RETaO_4$ (RE=La,Eu) polymorphs. Furthermore, multiple point analyses showed consistent La:Eu ratios throughout the samples. By lattice parameter refinement and visual inspection, we were also able to determine that 5–25% Eu substitution for La gave pure orthorhombic *Pbca* $LaTaO_4$:Eu, whereas higher concentration of Eu provided a mixture of phases. Both 35% and 40% Eu-substituted samples contained ~50% of the orthorhombic *Pbca* polymorph, and 50% of other rare-earth orthotantalate polymorphs discussed above. At these higher concentrations of Eu, the $LaTaO_4$:Eu mixture annealed at 900 °C still gives better QY than those annealed at 1150 °C (see Fig. 4), owed primarily to the portion of the mixture that is the *Pbca* polymorph. The phosphors annealed at 1150 °C do not contain any of the low-temperature polymorph. Unfortunately we were unable to obtain reliable La:Eu ratios of the RE-site via Rietveld refinement for any of the polymorphs, due to preferred orientation (see SEM images). This was especially true of phases featuring pure *Pbca* polymorph, in that these have a very elongated growth morphology.

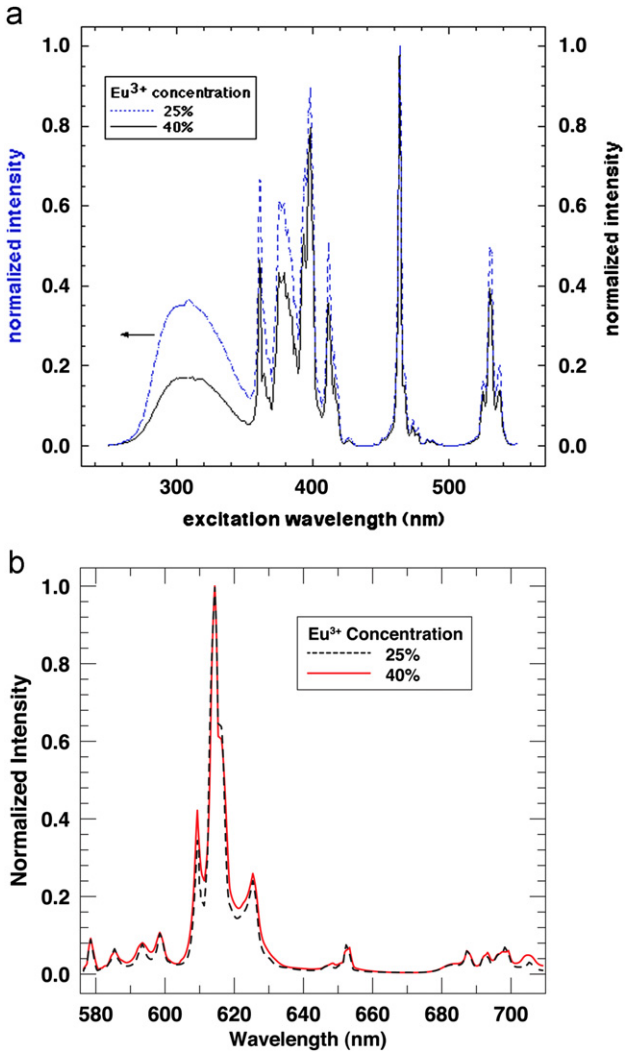

Fig. 6. (a) Excitation spectra of Eu^{3+}-doped $LaTaO_4$ polymorphs. The intensity of the Eu^{3+}–O^{2-} charge transfer band relative to the narrow 4*f* bands decreases with increasing Eu^{3+} concentration. (b). Emission spectra of Eu^{3+}-doped $LaTaO_4$ polymorphs excited at 464 nm.

Photoluminescence excitation and emission spectra for the different polymorphs are shown in Fig. 6(a and b). The excitation spectra of both polymorphs have a broad charge transfer (CT) band that peaks at ~300 nm, and narrow bands that denote the wavelengths at which the 4*f* transitions of Eu^{3+} can be excited directly. The most intense of these narrow bands is positioned at ~361, 398, and 464 nm. As shown in Fig. 6(a), the intensity of the CT band relative to that of the narrow bands decreases with increasing europium concentration. We attribute the CT band to Eu^{3+}–O^{2-} charge transfer rather than Ta^{5+}–O^{2-} charge transfer, because integrating sphere measurements of diffuse light absorbance show that Eu^{3+}-doped phosphors absorb appreciably more than undoped $LaTaO_4$. For example, one doped sample absorbed ~2.5 times more light at 310 nm and 3 times more light at 320 nm than the undoped sample. The emission spectra under 464 nm excitation, as shown in Fig. 6(b), have several narrow bands; the most intense of these is positioned at ~614 nm, and is due to the parity forbidden electric-dipole transition $^5D_0$–$^7F_2$. The $^5D_0$–$^7F_0$ transition at ~578 nm and the $^5D_0$–$^7F_1$ transition with peaks at ~585, 594, and 598 nm are less intense than the $^5D_0$–$^7F_2$ transition. This behavior is characteristic of phosphors in which the Eu^{3+} occupies sites that lack inversion symmetry [1]. Both $LaTaO_4$ polymorphs have non-centrosymmetric point groups [29].

The different polymorphs have similar excitation and emission spectra because of the inherent characteristic of *f*-orbitals in which the europium valence electrons reside. These electron orbitals are generally too low in energy to hybridize with host lattice orbitals. Therefore electron transitions between ground and excited states that are responsible for the red emission are not significantly affected by the host lattice. The most intense emission peak is at ~614 nm for both polymorphs. We examined the structural details for these polymorphs to determine whether site distortion introduced by the different polymorphs can be correlated with the quantum yield data.

The *Pbca* $LaTaO_4$:Eu polymorph has the best quantum yield across the Eu concentration range in which this polymorph is essentially pure (5–25%). The pertinent structural data summarized in Table 1 may help explain this result. The site symmetries based on crystallography, La–O distances, La–La distances, as well as the averaged La–La distance in the *Pbca*, $P2_1/c$ and $Cmc2_1$ $LaTaO_4$ polymorphs are listed in Table 1. In each polymorph, the La is bonded to eight oxygen ligands with bond lengths ranging from ~2.3–3.0 Å, and each LaO_8 polyhedron is edge-sharing with six LaO_8 polyhedra; in this regard, the three main polymorphs discussed in this paper are all very similar. Both the *Pbca* and $P2_1/c$ polymorphs have a rare-earth site symmetry of 1 (no symmetry

Table 1
Comparing La–La distances in $LaTaO_4$ polymorphs.

$LaTaO_4$ polymorph	*RE*-site multiplicity and Wyckoff position	Site symmetry	La–O distances (Å)	La–La distances (Å)	Average La–La distance (Å)
Pbca (#61) (low-temperature) [7]	8*c*	1	2.320–2.975	3.916(×2) 4.186(×2) 4.229(×1) 4.402(×1)	4.139
$P2_1/c$ (#14) [25]	4*e*	1	2.368–2.822	3.914(×2) 3.998(×1) 4.132(×2) 4.325(×1)	4.069
$Cmc2_1$ (#36) [26]	4*a*	*m*	2.304–2.939	3.931(×2) 4.168(×4)	4.089

operators) and the rare-earth site of the $Cmc2_1$ polymorph is of higher symmetry with a mirror plane (m). The listings of La–La bond distances provide further information about the site symmetry. The average La–La distance is longest for the *Pbca* polymorph. The longer distance may serve to minimize concentration quenching, but this is not the dominating factor that limits QY in these materials. The $Cmc2_1$ polymorph has two different La–O distances, and the LaO_8 polyhedra of the *Pbca* and $P2_1/c$ polymorphs each have four different La–O distances. In comparing the LaO_8 polyhedra of the two latter polymorphs, the *Pbca* phase has a wider range of La–O bond distances (see Table 1), and thus is even more distorted. Of course we do not know the exact metric parameters for the analogous Eu-substituted polymorphs, but we can probably assume that they follow the same trends as those outlined in Table 1. To summarize, examination of the *RE*-site in these polymorphs reveals the *Pbca* polymorph that give the highest Eu-QY also has the most distorted *RE*-site, and there may be a form-function correlation.

The morphologies of the 25%-Eu substituted $LaTaO_4$:Eu materials from the three different processing methods are illustrated in Fig. 7. The morphologies of $LaTaO_4$:Eu from solid-state processing and from annealing $La_2Ta_2O_7(OH)_2$:Eu at 1150 °C are quite similar; they were both annealed as pellets and at the same temperature. On the other hand, $LaTaO_4$:Eu from annealing $La_2Ta_2O_7(OH)_2$:Eu at 900 °C preserves the crystalline morphology of the $La_2Ta_2O_7(OH)_2$:Eu precursor. This morphology can be described as similar to planks. Fig. 7d shows 40%-Eu substituted $LaTaO_4$:Eu from annealing $La_2Ta_2O_7(OH)_2$:Eu at 900 °C. While the plank-like morphology of orthorhombic *Pbca* 25%-Eu substituted $LaTaO_4$:Eu is observed, we observe smaller needles that are clustered in bowtie-shaped bundles are also present in equal abundance. These are likely composed of the other rare-earth tantalate polymorphs.

Finally, we investigated the effect of annealing time at 900 °C on stability of the *Pbca* $RETaO_4$ polymorph, QY and morphology; and these results are summarized in Fig. 8. For the 30% Eu-substituted $LaTaO_4$, extensive heating time resulted in decreased QY, approximately 10% decrease per day of heating. We observe both by SEM imaging and powder X-ray diffraction an alteration in morphology. The sample annealed for 2 h at 900 °C has morphology that reflects that of the $RE_2Ta_2O_7(OH)_2$ morphology, with preferential growth on the (0*kl*) plane. Upon annealing for 48 h at 900 °C, we see decrease in the (022) and (033) peaks in particular and correlated relative increase in the other peak intensities (see Fig. 8). By SEM, we see first a 'splintering' of the ends of the elongated crystals, and then annealing together and finally breaking off in triangular-shaped pieces (Fig. 8). These morphology changes are consistent with the decrease in preferred orientation observed in X-ray powder diffraction patterns. The triangular-shaped pieces have a more globular appearance, similar to those $RETaO_4$ powders produced by high-temperature solid-state processing, shown in Fig. 7. However, there is no evidence for polymorph change; the *Pbca* phase still dominates. This study reveals provides several insights. The *Pbca* polymorph is stable at

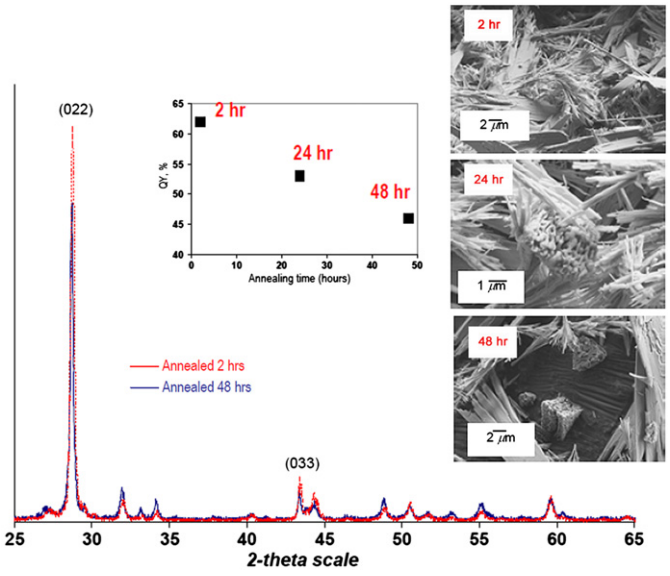

Fig. 8. Effect of annealing time on QY, morphology and phase of 30%-Eu substituted *Pbca* $LaTaO_4$. Annealing temperature is 900 °C (see text).

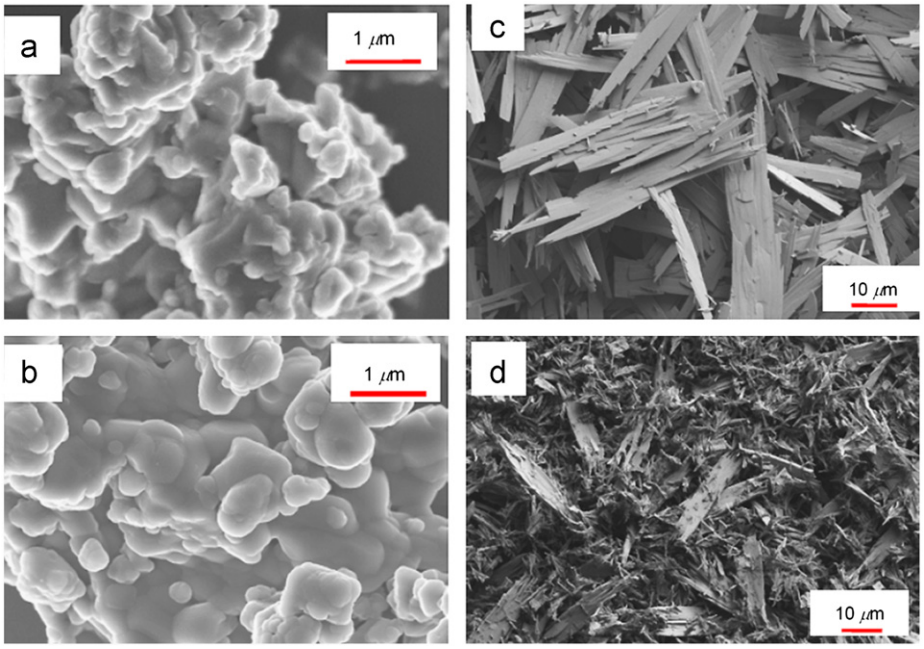

Fig. 7. 25%-Eu substituted $LaTaO_4$:Eu. (a) from solid-state processing at 1150 °C, (b) from $La_2Ta_2O_7(OH)_2$:Eu precursor annealed at 1150 °C, and (c) from $La_2Ta_2O_7(OH)_2$:Eu precursor annealed at 900 °C. (d) 40%-Eu substituted $LaTaO_4$:Eu from $La_2Ta_2O_7(OH)_2$:Eu precursor annealed at 900 °C.

900 °C, even with prolonged heating. The QY is a more sensitive indicator of subtle chemical and physical characteristics (i.e. morphology change) of the phosphor than other methods of characterization. The decrease in QY is likely a result of defect formation that accompanies the morphology change, and is not readily detected by most bulk characterizations. This study summarized in Fig. 8 is an example of how systematic studies (i.e. effect of dopant concentration on QY) on phosphor materials are very challenging, in that one change can have multiple effects that cannot necessarily be readily detected.

4. Conclusions

Correlation of Eu quantum-yield with Eu-concentration in $LaTaO_4$:Eu materials is not straight-forward. There are multiple $RETaO_4$ polymorphs, and the dominant polymorph changes as a function of RE-radius, directly related to La:Eu ratio. In this study, we have shown the QY is limited not by concentration quenching, but by the maximum Eu-concentration which gives pure *Pbca* $RETaO_4$ polymorph (83% QY at 25% Eu-substitution). Above the optimal Eu-concentration of 25%, other polymorphs form and the QY drops to around 60%. By comparing the RE-coordination in the different $RETaO_4$ polymorphs, we have concluded the lowest symmetry of the REO_8 polyhedron may be responsible for the highest Eu QY in the *Pbca* polymorph. Moreover, the *Pbca* polymorph can only be obtained by annealing the $(RE)_2Ta_2O_7(OH)_2$ precursor at 900 °C. Both higher temperature annealing and traditional solid-state processing give different polymorphs with lower QY. Additionally, solid-state synthesis of $RETaO_4$ requires processing temperatures in excess of 1600 °C, nearly double that than the process reported here, to obtain comparable crystallinity and phase-purity. Therefore, this study gives a clear example where 'soft-chemistry' distinctly provides optimal function from material form that is unique to the synthesis technique.

Acknowledgments

This work was supported by Sandia's Solid-State-Lighting Science Energy Frontier Research Center, funded by the U.S. Department of Energy, Office of Science, Office of Basic Energy Sciences. Sandia National Laboratories is a multi-program laboratory managed and operated by Sandia Corporation, a wholly owned subsidiary of Lockheed Martin Corporation, for the U.S. Department of Energy's National Nuclear Security Administration. We thank Gary L. Zender (SNL) for the SEM-EDS analyses.

References

[1] S. Shionoya, W.M. Yen, Phosphor Handbook, in: M.J. Weber (Ed.), Laser and Optical Science and Technology Series, CRC Press, Boca Raton, 1999.
[2] Y. Fang, Y.Q. Li, T. Qiu, A.C.A. Delsing, G. de With, H.T. Hintzen, J. Alloy Compd. 496 (2010) 614–619.
[3] Y.Q. Li, C.M. Fang, Y. Fang, A.C.A. Delsing, G. de With, H.T. Hintzen, J. Solid State Chem. 182 (2009) 3299–3304.
[4] Y.Q. Li, A.C.A. Delsing, R. Metslaar, G. de With, H.T. Hintzen, J. Alloy Compd. 487 (2009) 28–33.
[5] Y.Q. Li, J.E.J. van Steen, J.W.H. van Krevel, G. Botty, A.C.A. Delsing, F.J. DiSalvo, G. de With, H.T. Hintzen, J. Alloy Compd. 417 (2006) 273–279.
[6] Y.Q. Li, A.C.A. Delsing, G. de With, H.T. Hintzen, Chem. Mater. 17 (2005) 3242–3248.
[7] M. Nyman, M.A. Rodriguez, L.E.S. Rohwer, J.E. Martin, M. Waller, F.E. Osterloh, Chem. Mater. 21 (2009) 4731–4737.
[8] M. Nyman, M.A. Rodriguez, L.E. Shea-Rohwer, J.E. Martin, P.P. Provencio, J. Am. Chem. Soc. 131 (2009) 11652.
[9] I.P. Roof, M.D. Smith, S. Park, H.C. zur Loye, J. Am. Chem. Soc. 131 (2009) 4202.
[10] M. Thomas, P.P. Rao, M. Deepa, M.R. Chandran, P. Koshy, J. Solid State Chem. 182 (2009) 203–207.
[11] X.Z. Xiao, B. Yan, J. Mater. Res. 23 (2008) 679–687.
[12] K.S. Hwang, B.A. Kang, S. Hwangbo, Y.S. Kim, J.T. Kim, Electron. Mater. Lett. 6 (2010) 27–30.
[13] P.P. Dai, X.T. Zhang, X.H. Li, G.R. Wang, C.J. Zhao, Y.C. Liu, J. Lumin. 131 (2011) 653–656.
[14] M.A. Ryumin, V.V. Pukhkaya, L.N. Komissarova, Russ. J. Inorg. Chem. 55 (2010) 1010–1013.
[15] Q.Y. Shao, H.J. Li, K.W. Wu, Y. Dong, J.Q. Jiang, J. Lumin. 129 (2009) 879–883.
[16] Y.R. Do, Y.D. Huh, J. Electrochem. Soc. 147 (2000) 4385–4388.
[17] T.C. Jagau, I.P. Roof, M.D. Smith, H.C. zur Loye, Inorg. Chem. 48 (2009) 8220–8226.
[18] I.P. Roof, T.C. Jagau, W.G. Zeier, M.D. Smith, H.C. zur Loye, Chem. Mater. 21 (2009) 1955–1961.
[19] C.H. Chiu, C.H. Liu, S.B. Huang, T.M. Chen, J. Electrochem. Soc. 155 (2008) J71–J78.
[20] J. Pan, L.Z. Yau, L.G. Chen, G.W. Zhao, G.E. Zhou, C.X. Guo, J. Lumin. 40–1 (1988) 856–857.
[21] M. Nyman, M.A. Rodriguez, T.M. Alam, T.M. Anderson, A. Ambrosini, Chem. Mater. 21 (2009) 2201–2208.
[22] T.Z. Forbes, M. Nyman, M.A. Rodriguez, A. Navrotsky, J. Solid State Chem. 183 (2010) 2516–2521.
[23] T.M. Anderson, M.A. Rodriguez, F. Bonhomme, J.N. Bixler, T.M. Alam, M. Nyman, Dalton T, (2007) 4517–4522.
[24] L.S. Rohwer, J.E. Martin, J. Lumin. 115 (2005) 77–90.
[25] I. Hartenbach, F. Lissner, T. Nikelski, S.F. Meier, H. Muller-Bunz, T. Schleid, Z. Anorg. Allg. Chem. 631 (2005) 2377–2382.
[26] M.S. Slobodyanik, A.O. Kapshuk, N.M. Belyavina, V.Y. Markiv, A.M. Sich, Y.O. Titov, Dopov. Nats. Akad. Ukr (2003) 140–145.
[27] R.J. Cava, R.S. Roth, J. Solid State Chem. 36 (1981) 139–147.
[28] R.D. Shannon, Acta Crystallogr. A 32 (1976) 751–767.
[29] K. Binnemans, C. Gorller-Walrand, J. Rare Earths 14 (3) (1996) 173–180.